Effects of thickness on switching current for $(Pb_{0.97}La_{0.02})(Zr_{0.95}Ti_{0.05})O_3$ antiferroelectric films under thermo-electric coupled field

Kun An[1], Erwei Wang[2], Jian He[2], Xiujian Chou[2] ✉, Chenyang Xue[2], Wendong Zhang[2]

[1]*School of Computer Science and Control Engineering, North University of China, Taiyuan 030051, People's Republic of China*
[2]*National Key Laboratory for Electronic Measurement Technology, North University of China, Taiyuan 030051, People's Republic of China*
✉ *E-mail: chouxiujian@nuc.edu.cn*

Published in Micro & Nano Letters; Received on 12th February 2016; Revised on 21st April 2016; Accepted on 26th April 2016

Homogeneous and compact antiferroelectric (AFE) (Pb, La)(Zr, Ti)O_3 thick films in large area with different thicknesses were successfully fabricated by the sol–gel processing on Pt(111)/Ti/SiO_2/Si(100) substrates. The characteristics of switching current of samples with different thicknesses under thermo-electric coupled field were investigated in detail. The experimental result shows that the peak of switching current density increased with the increase of temperature in three samples. Moreover, it is found that the thickness of the films has a big effect on the current density. Therefore, the peak of switching current density increased with increasing in the thickness at the same temperatures. The maximum switching current density of film with the thickness of 2254 nm is 4.35×10^{-5}A/cm^2. These results are quite important and necessary for design and preparation of the AFE materials applied on high sensitivity and intelligent micro-sensors and micro-actuators.

1. Introduction: With the rapid development of MEMS, more and more micro-/nano- devices have been widely employed in military and civil products. For many micro and nano devices, there is not a single physical field to apply in, but multi-physical fields in the fields of practical engineering, the aerospace and the navigation [1–3], e.g. the temperature field, the stress field, the electric field, the magnetic field etc. Therefore, the coupled effects of multi-physical fields can be paid more attentions to, especially the design and preparation of micro and nano devices [4]. It can not only reveal the kinetical characteristics of MEMS devices and the response patterns with multiple factors to optimise the structure, but also improve the effectiveness and feasibility of the practical applications [5–7].

Considering so many MEMS devices are fabricated by films or bulk [8–10], the thickness of films or bulk is a really important factor to influence the electrical properties of materials, such as the material density, the polarisation characteristics, the phase switching field, the dielectric constant and dielectric loss, the coercive field [11–14]. However, there are few reports, to the best of our knowledge, about the effects of the antiferroelectric (AFE) films thickness on the switching current under thermo-electric coupled field.

AFE materials can indicate a special property of electric-field-induced phase transformation from AFE to ferroelectric (FE), accompanying with remarkable changes in the dielectric constant, polarisation and current owing to the crystal structure. This process causes a great transition strain effect with a fast speed of phase transformation, and it can be regulated easily by either the temperature or the hydrostatic pressure.

Currently, there are about 40 kinds of the AFE material [15, 16], in which $PbZrO_3$-based AFE material is considered to be a kind of the most promising materials and becomes one of the most important objects in AFE material studies [17, 18], due to its simple structure and excellent performance. Hence, the effects of the switching current of $(Pb_{0.97}La_{0.02})(Zr_{0.95}Ti_{0.05})O_3$ (PLZT) AFE thick films with different thicknesses under the thermo-electric coupled field were explored systematically subsequent to our previous studies in this Letter. It is necessary to optimise the structure of PLZT AFE thick films for wide application prospects in the fields of micro-sensors and micro-actuators.

2. Preparation of thick films: $(Pb_{0.97}La_{0.02})(Zr_{0.95}Ti_{0.05})O_3$ AFE thick films were prepared by sol–gel method, which was similar to our previous works [19, 20]. $[Pb(CH_3COO)_2{\cdot}3H_2O]$, $[La(CH_3COO)_3{\cdot}H_2O]$, $[Zr(OC_3H_7)_4]$ and $[Ti[OCH(CH_3)_2]_4]$ were selected as the raw materials. First, the raw materials were mixed in a ration of lead acetate trihydrate with 15 mol% excess, lanthanum acetate hydrate, acetic acid and distilled at 110°C for 60 min; second, Zirconium propoxide and titanium isopropoxide were added and mixed for 30 min until the mixed solution was cooled to room temperature. During the mixing process, distilled water was added in the proportion of 20 mol of distilled water to 1 mol of lead in order to stabilise the solution. To improve the properties of the films, lactic acid and ethylene glycol as the stable and polymerising agents were added into the solution; finally, the solution was adjusted to 0.3 mol using acetic acid. After 24 h, $(Pb_{0.97}La_{0.02})(Zr_{0.95}Ti_{0.05})O_3$ thick films were grown on the substrates by a multiple-layer spin-coating process. The spin coating and heat-treatment were repeated for many times to crystallise into the perovskite phase, which is the type of crystalline form and brings out the strong AFE traits. The Au top electrodes with 0.5 mm in diameter of three samples were chosen in this work.

3. Characterisations: Cross sectional morphological features of the films are examined by the scanning electron microscopy (SEM). Gold pads of 0.5 mm in diameter were obtained on the film surfaces as top electrodes by DC sputtering for the electrical measurement. The *P* (polarisation)-*E*(electric field) loops were measured by a modified Sawyer-Tower circuit. Current density (electric-field intensity)-time curves were investigated by the Keithley 6517A electrometer. The test circuit diagram of the switching current under thermo-electric coupled field is shown in Fig. 1.

4. Results and discussions: The films with different thickness were determined by cross sectional SEM image, shown in Fig. 2. These results indicate that the formation of PLZT thick films is well coated on surface of silicon substrate. All the films have homogeneous thicknesses: about 1054.0, 1500.0 and 2254.0 nm corresponding to samples A, B and C, respectively.

doi: 10.1049/mnl.2016.0040

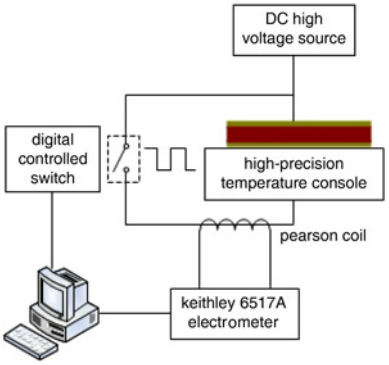

Fig. 1 *Test circuit diagram of the switching current under thermo-electric coupled field*

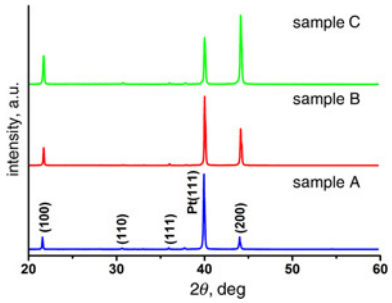

Fig. 3 *XRD patterns of PLZT thick films of different thicknesses grown on the Pt (111)/Ti/SiO2/Si substrate*

Fig. 3 shows the X-ray diffraction patterns of the PLZT AFE thick films with different thicknesses. All samples show four diffraction peaks at $2\theta = 22°$, 31°, 38°, 40° and 44° with no other diffraction peaks, corresponding to (100), (110), (111), and (200) orientations of PLZT, respectively. These results indicate the

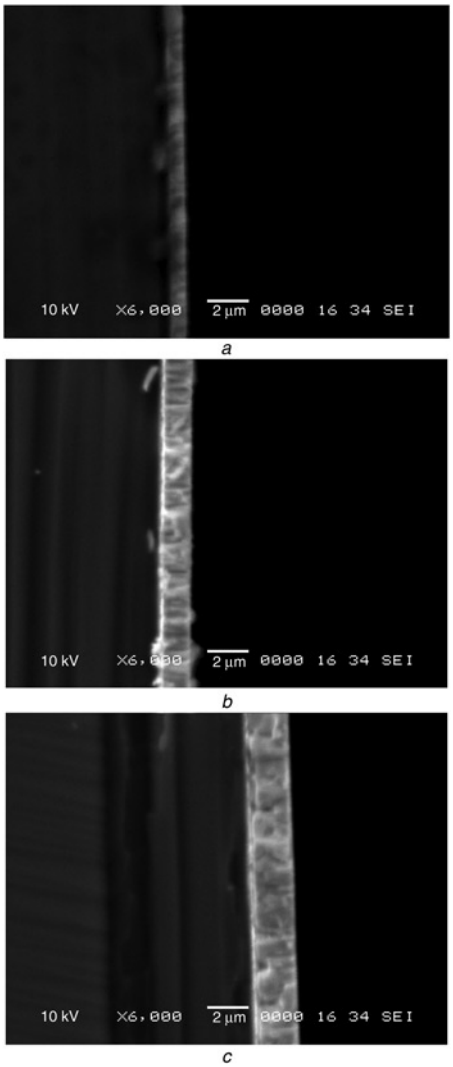

Fig. 2 *Cross-section SEM images for PLZT thick films with different thickness*
a Sample A
b Sample B
c Sample C

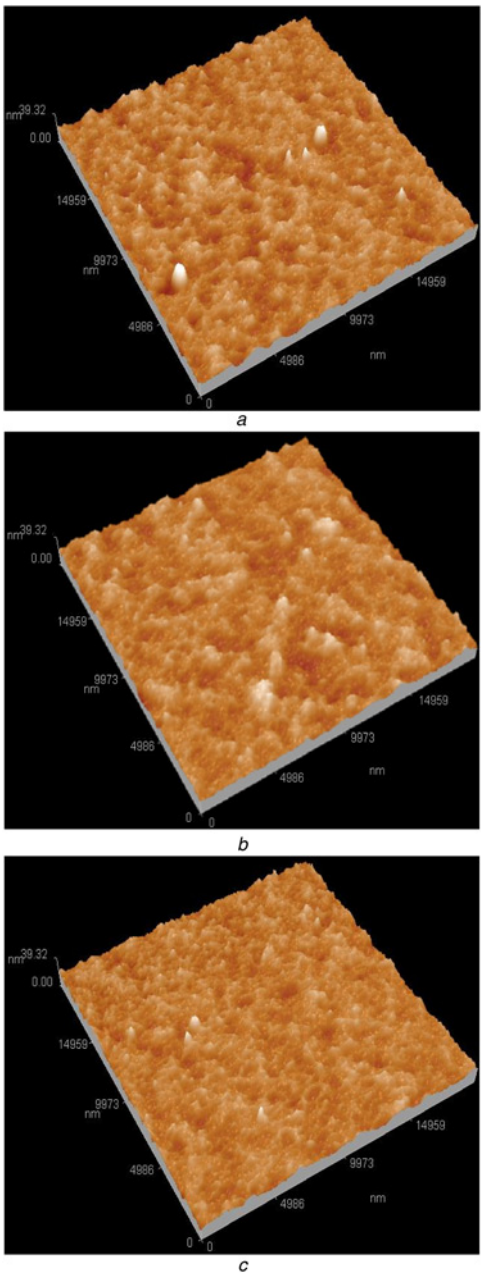

Fig. 4 *3D-AFM images for PLZT thick films at different thickness*
a Sample A
b Sample B
c Sample C

formation of PLZT AFE thick films with different thicknesses. It is also clearly seen that the ratios of (100) and (200) diffraction intensity increase with the increase of the thickness, while the diffraction intensity of Pt (111) shows the opposite trend. It is well known that the film thickness is one of important factors for its orientation.

The AFM images in Fig. 4 show the morphology of PLZT films with different thicknesses. The surface of the films is dense, without cracks or voids. The roughnesses of films are about 2.11, 1.89 and 1.76 nm with different thicknesses. Based on these results, it can be further concluded that the PLZT films with different thicknesses are successively prepared, while the surface morphology does not notably change when increasing the film thickness.

The *P-E* curves of PLZT thick films with different thicknesses are shown in Fig. 5. The double hysteresis loops of all samples presented above are squared-like of $(Pb_{0.97}La_{0.02})(Zr_{0.95}Ti_{0.05})O_3$ thick films, indicating the AFE nature at room temperature. The *P-E* loops represent the abrupt increases in polarisation and sharp phase switching between the phases of AFE and FE. Films with different thicknesses have a relatively small remnant polarisation at zero electric field. The saturation polarisations are 45.67, 46.46 and 48.63 $\mu C/cm^2$ corresponding to the samples A, B and C, respectively. The result indicates the saturated polarisations increase with the increase of thicknesses of the films. The switch fields can be also estimated by their intersections with the horizontal axis the when extrapolating two steepest sections of the *P-E* loops. The forward (AFE-to-FE) phase switch fields E_F are 170, 180 and 200 kV/cm, respectively. Obviously, the values of both forward phase switching fields (E_F) and backward (FE-to-AFE) ones (E_A) increase with the thickness increase. A small amount of remnant polarisation (P) of the films may result from the leakage and the stress of substrates, and decrease oppositely when increasing the thickness.

To observe the change of switching current due to transforming phase, the J (current density)-T (time) and E (electric field)-T (time) curves of PLZT thick films with different thicknesses under various temperatures are measured in Fig. 6. The measurement was conducted in the way of $-E_{max}$ to 0 and then E_{max} to 0. The forcing time was 5 s. The time delay between the field change and the data acquisition was 5 s, too. The J–T curves show obvious switching current peaks of AFE to FE and FE to AFE with the direction change of voltage during the cycle test process. The switching current density of samples A, B and C, described in more detail are summarised in Tables 1–3. The switching current can be involved in three parts. The first part comes from the phase transformation current of AFE to FE or FE to AFE that has a little decrease when the temperature is increasing, because the polarised energy of phase transformation was released in advance when increasing the temperature. The second part is from the pyroelectric current that increases with the increase of the temperature. The last part is the leakage current that is quite small and may be neglected owing to the high quality of the film in all samples.

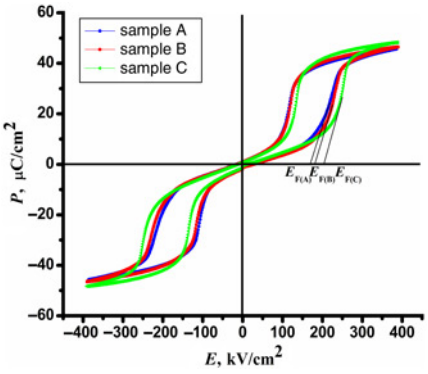

Fig. 5 *P(polarisation)-E(electric field) curves of PLZT AFE thick films with different thickness at room temperatures*

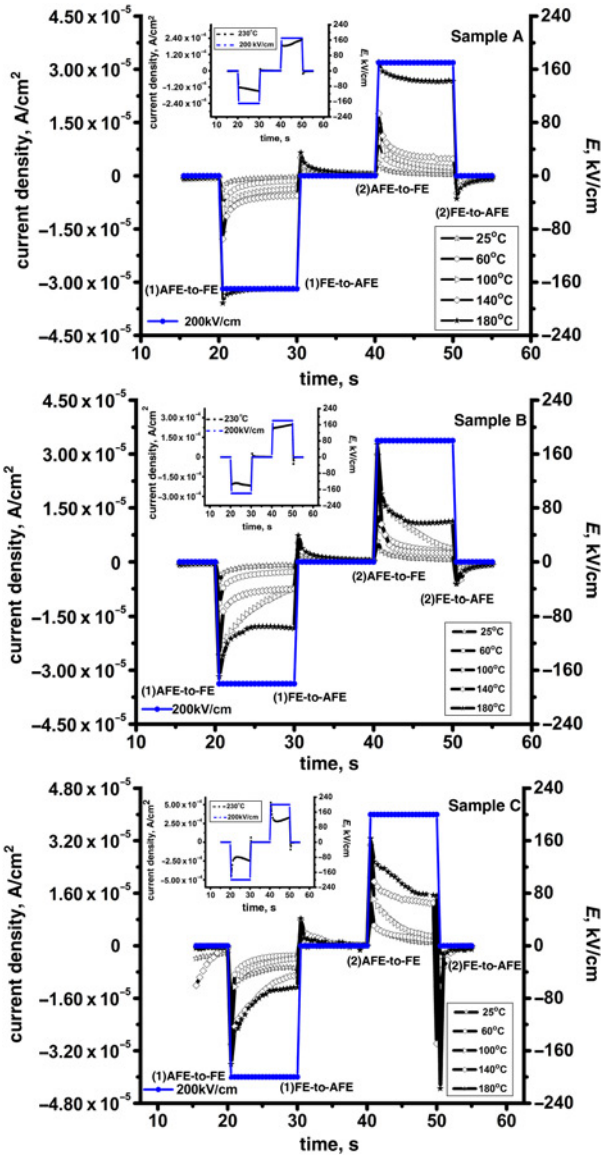

Fig. 6 *J(current density) –T(time) and E(electric field) –T(time) curves of PLZT AFE thick films under various temperature with different thickness*

When the applied electric field is greater than the threshold, the dipoles are polarised, where the adjacent sublattice dipoles orient in the same directions of the electric field form the significant current during the process of AFE-to-FE phase transition. In the

Table 1 Phase transition current density of PLZT AFE thick film under various temperatures for sample A

Temp.	The first period		The second period	
T (°C)	$J_{AFE\rightarrow FE}$ (A/cm^2)	$J_{FE\rightarrow AFE}$ (A/cm^2)	$J_{AFE\rightarrow FE}$ (A/cm^2)	$J_{FE\rightarrow AFE}$ (A/cm^2)
25	-3.9×10^{-6}	1.2×10^{-6}	3.61×10^{-6}	-1.24×10^{-6}
60	-7.92×10^{-6}	2.42×10^{-6}	9.46×10^{-6}	-2.1×10^{-6}
100	-1.58×10^{-5}	4.15×10^{-6}	1.47×10^{-5}	-2.92×10^{-6}
140	-1.78×10^{-5}	5.15×10^{-6}	1.75×10^{-5}	-4.91×10^{-6}
180	-3.18×10^{-5}	6.53×10^{-6}	3.20×10^{-5}	-6.11×10^{-6}
230	-1.22×10^{-4}	1.23×10^{-5}	1.90×10^{-4}	-2.15×10^{-5}

doi: 10.1049/mnl.2016.0040

Table 2 Phase transition current density of PLZT AFE thick film under various temperatures for sample B

Temp.	The first period		The second period	
T (°C)	$J_{AFE\rightarrow FE}$ (A/cm^2)	$J_{AFE\rightarrow FE}$ (A/cm^2)	$J_{FE\rightarrow AFE}$ (A/cm^2)	$J_{FE\rightarrow AFE}$ (A/cm^2)
25	-5.56×10^{-6}	1.58×10^{-6}	5.71×10^{-6}	-2.49×10^{-6}
60	-1.14×10^{-5}	3.31×10^{-6}	1.36×10^{-5}	-3.25×10^{-6}
100	-2.35×10^{-5}	4.18×10^{-6}	2.24×10^{-5}	-3.39×10^{-6}
140	-2.56×10^{-5}	5.29×10^{-6}	2.99×10^{-5}	-5.93×10^{-6}
180	-3.59×10^{-5}	7.31×10^{-6}	3.26×10^{-5}	-6.42×10^{-6}
230	-2.09×10^{-4}	2.52×10^{-5}	2.10×10^{-4}	-5.19×10^{-5}

Table 3 Phase transition current density of PLZT AFE thick film under various temperatures for sample C

Temp.	The first period		The second period	
T (°C)	$J_{AFE\rightarrow FE}$ (A/cm^2)	$J_{AFE\rightarrow FE}$ (A/cm^2)	$J_{FE\rightarrow AFE}$ (A/cm^2)	$J_{FE\rightarrow AFE}$ (A/cm^2)
25	-1.84×10^{-5}	2.61×10^{-6}	9.06×10^{-6}	-3.18×10^{-6}
60	-2.08×10^{-5}	3.60×10^{-6}	1.41×10^{-5}	-3.68×10^{-6}
100	-2.78×10^{-5}	4.48×10^{-6}	2.68×10^{-5}	-5.37×10^{-6}
140	-3.0×10^{-5}	7.9×10^{-6}	3.07×10^{-5}	-2.98×10^{-5}
180	-3.61×10^{-5}	8.27×10^{-6}	3.27×10^{-5}	-4.35×10^{-5}
230	-4.41×10^{-4}	6.24×10^{-5}	5.27×10^{-4}	-9.64×10^{-5}

same way, when the applied electric field is less than the threshold, the dipoles are depolarised during the FE-to-AFE phase transition process. AFE changes phase between AFE and FE alternatively with or without electric field. The dipoles oriented in the same directions of the negative electric field and crystals are induced to ferroelectrics under the applied negative electric field; when the negative voltage is suddenly removed, the dipoles are depolarised and re-back to the lower energy state and form the significant current peak, whose direction is opposite to that of AFE to FE. Therefore, the conversion principle of AFE and FE is the case under the applied positive electric field.

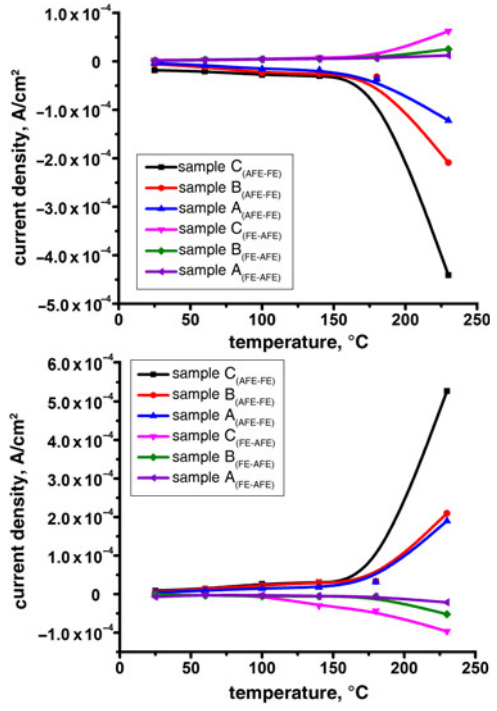

Fig. 7 *J (current density)-T (temperature) curves of PLZT AFE thick films with different layers from 25°C to 230°C*

The switching current increases with the increase of the temperature in all cases because the adding pyro-electric currents are much larger than the decreasing phase transformation current. The peak current of PLZT thick films at 230°C is obviously higher than that below 230°C in all samples. Consequently, the peak current is the leakage current, instead of the transition phase one, because the AFE phase of films are induced to the PE phase. The maximum switching current is -4.35×10^{-5}A/cm^2 under the thermo-electric coupled field, which comes from sample C.

The current is instantaneous and the current density is big in the courses of polarisation and depolarisation, because the transformation processes from AFE to FE and from FE to AFE are as short as nanosecond order of magnitude. AFE can exhibit several phase transformations among AFE, FE and PE and the direction of polarisation with the change of transformation process when the change of environmental temperature, that causes strong peak of phase transition current. The temperature and the peak intensity of phase transition can be controlled by selecting components. Fig. 6 shows that the electric fields have the same directions with both the leakage and the phase current from AFE to FE during the polarisation process. The electric fields have the same directions with the leakage but opposite the phase current from FE to AFE during the depolarisation process.

To observe the change of switching current owing to transforming phase, the J–T curves of different thicknesses of PLZT thick films under various temperatures from 25°C to 230°C are measured in Fig. 7. It should be noted that the switching current of sample C is always the largest one under the temperatures from 25°C to 230°C during two periods, because the thickness of sample C is higher than those of samples A and B. It is illustrated from Tables 1–3 that the peak of the switching current density increases with increase of the thickness at the same temperature.

Fig. 7*a* shows that the switching current of sample C (the black curve) is the largest one and up to 3.61×10^{-5} A/cm^2 during the phase transformation from AFE to FE. The switching current of sample C is the largest one and up to 8.27×10^{-6} A/cm^2 during the phase transformation from FE to AFE at the same temperature. Fig. 7*b* is the same law with Fig. 7*a*, but the switching current direction is different. In other words, the thickness of the AFE thick film is one of the important indicators of the energy storage.

5. Conclusion: The AFE thick films of PLZT ($Pb_{0.97}La_{0.02}Zr_{0.95}Ti_{0.05}O_3$) were prepared on Pt (111)/Ti/SiO_2/Si (100) substrates by the sol–gel processing with the different thicknesses of samples A, B and C, respectively. The switching current of PLZT AFE thick films with the different thicknesses under the thermo-electric coupled field were investigated in detail. From J–T and E–T curves, two periods of phase transition can be observed from AFE to FE and from FE to AFE, where the switching current densities increase with the increase of the temperatures in all cases. The maximum current density from sample A is 4.35×10^{-5} A/cm^2 under the thermo-electric coupled field. The peak of switching current density increases when increasing in the thickness at the same temperature. These results are quite important for the AFE materials applied in high sensitivity and intelligent sensor MEMS devices.

6. Acknowledgements: This work was supported by National Natural Science Foundation of China under grant nos. 61401406 and 51422510, Program for New Century Excellent Talents in

University of China (NCET) and Functional Materials Research Laboratory, Tongji University, China.

7 References

[1] Wang T.Z., Zhou Y.H.: 'Nonlinear dynamic model with multi-fields coupling effects for giant magnetostrictive actuators', *Int. J. Solids Struct.*, 2013, **50**, pp. 2970–2979

[2] Sun Y.G., Yao X.H., Han Q.: 'Combined torsional buckling of double-walled carbon nanotubes with axial load in the multi-field coupled condition', *Sci. China Phys. Mech. Astron.*, 2011, **54**, pp. 1659–1665

[3] Yang L., Zhang S.P., Zhang G.Z., *ET AL.*: 'Specially environmental responses induced by multi-field coupling for nanocrystalline SnO_2 porous film as gas sensor', *Sens. Actuators B Chem.*, 2013, **182**, pp. 239–249

[4] Xu L.Z., Yang Q.: 'Multi-Field coupled dynamics for a micro beam', *Mech. Based Des. Struct. Mach.*, 2015, **43**, pp. 57–73

[5] Saad N.H., Al-Dadah R.K.: 'Analysis of MEMS mechanical spring for coupling multimodal micro resonators sensor', *Microelectron. Eng.*, 2009, **86**, pp. 1190–1193

[6] Forke R., Scheibner D., Mehner J.E.: 'Electrostatic force coupling of MEMS oscillators for spectral vibration measurements', *Sens. Actuators A Phys.*, 2008, **142**, pp. 276–283

[7] Zhang Z.Q., Liao X.P., Han L.: 'A coupling RF MEMS power sensor based on GaAsMMIC technology', *Sens. Actuators A Phys.*, 2010, **160**, pp. 42–47

[8] Cook-Chennault K.A., Thambi N., Sastry A.M.: 'Powering MEMS portable devices a review of non regenerative and regenerative power supply systems with special emphasis on piezoelectric energy harvesting systems', *Smart Mater. Struct.*, 2008, **17**, p. 043001

[9] Elfrink R., Kamel T.M., Goedbloed M., *ET AL.*: 'Vibration energy harvesting with aluminum nitride-based piezoelectric devices', *J. Micromech. Microeng.*, 2009, **19**, p. 094005

[10] Cross L.E., Trolier-McKinstry S.: 'Thin film integrated ferroelectrics', *Encycl. Appl. Phys.*, 1997, **21**, pp. 429–451

[11] Chou X.J., Guo M.X., Zhang Y.T., *ET AL.*: 'Preparation and dielectric properties of highly preferrend-(100) orientation (Pb, La)(Zr, Ti)O_3 antiferroelectreic thick films by sol-gel precessing', *J. Sol-Gel Sci. Technol.*, 2012, **61**, pp. 62–68

[12] Liu J., Liu E.X., Zhang T.H., *ET AL.*: 'Thickness dependence of two-dimensional photonic quasicrystal lens imaging characteristics', *Solid State Commun.*, 2005, **201**, pp. 68–71

[13] Hao X.H., Zhai J.W., Zhou F.: 'Thickness and frequency dependence of electric-field-induced strains of sol-gel derived $(Pb_{0.97}La_{0.02})(Zr_{0.95}Ti_{0.05})O_3$ antiferroelectric films', *J. Sol-Gel Sci. Technol.*, 2010, **53**, pp. 366–371

[14] Yap C.C., Yahaya M., Salleh M.M.: 'Influence of thickness of functional layer on performance of organic salt-doped OLED with ITO/PVK: PBD: TBAPF6/A1 structure', *Cur. Appl. Phys.*, 2008, **8**, pp. 35–39

[15] Yasuda N., Konda J.: 'Successive paraelectric-antiferro-electric-ferroelectric phase transitions in highly ordered perovskite lead ytterbium tantalite', *Appl. Phys. Lett.*, 1993, **62**, pp. 535–537

[16] Barbur I., Ardelean I.: 'Electron paramagnetic resonance study of paramagnetic centres in antiferroelectric Pb2MgWO6', *J. Mater. Sci. Lett.*, 1993, **12**, pp. 1747–1748

[17] Geng W.P., Liu Y., Meng X.J., *ET AL.*: 'Giant negative electrocaloric effect in antiferroelectric La doped $Pb(ZrTi)O_3$ thin films near room temperature', *Adv. Mater.*, 2015, **27**, pp. 3165–3169

[18] Hao X.H., Zhai J.W., Kong L.B., *ET AL.*: 'A comprehensive review on the progress of lead zirconate-based antiferroelectric materials', *Prog. Mater. Sci.*, 2014, **63**, pp. 1–57

[19] Geng W.P., Chou X.J., Lv Y.B., *ET AL.*: 'Preparation and dielectric properties of (Pb, La)(Zr, Ti)O_3 antiferroelectric thick films on silicon substrates', *Electron. Compon. Mater.*, 2012, **31**, pp. 35–39

[20] Chou X.J., Geng W.P., Lv Y.B., *ET AL.*: 'Direct current electric field adjustable phase transformation behavior in (Pb,La)(Zr,Ti)O_3 antiferroelectric thick films', *J. Mater. Sci. Mater. Electron.*, 2013, **24**, pp. 4522–4527

doi: 10.1049/mnl.2016.0040